

# Re-evaluation of initial bone mineralization from an engineering perspective

Emilio Satoshi Hara, DDS, PhD,<sup>1</sup> Masahiro Okada, PhD,<sup>1</sup> Noriyuki Nagaoka, PhD,<sup>2</sup> Takayoshi Nakano, PhD,<sup>3</sup> Takuya Matsumoto, DDS, PhD,<sup>1</sup>

<sup>1</sup> Department of Biomaterials, Graduate School of Medicine, Dentistry and Pharmaceutical Sciences, Okayama University, 2-5-1 Shikata-Cho, Okayama, 700-8558 Japan. Tel: +81-86-235-6667. Fax: +81-86-6669.

<sup>2</sup> Advanced Research Center for Oral & Craniofacial Sciences, Graduate School of Medicine, Dentistry and Pharmaceutical Sciences, Okayama University, 2-5-1 Shikata-Cho, Okayama, 700-8558 Japan. Tel: +81-86-235-6667. Fax: +81-86-6669.

<sup>3</sup> Division of Materials and Manufacturing Science, Graduate School of Engineering, Osaka University, 2-1 Yamadaoka, Suita, Osaka, 565-0871, Japan. Tel and Fax: +81-6-6879-7506.

Emilio Satoshi Hara, DDS, PhD : gmd421209@s.okayama-u.ac.jp

Masahiro Okada, PhD : m\_okada@cc.okayama-u.ac.jp

Noriyuki Nagaoka, PhD : nagaoka@okayama-u.ac.jp

Takayoshi Nakano, PhD : nakano@mat.eng.osaka-u.ac.jp

Takuya Matsumoto, DDS, PhD : tmatsu@md.okayama-u.ac.jp

\*Address correspondence to:

Takuya Matsumoto, DDS, PhD.

Professor and Chair

Department of Biomaterials

Okayama University Graduate School of Medicine, Dentistry and Pharmaceutical Sciences, 2-5-1 Shikata-cho, Kita-ku, Okayama, 700-8558, Japan.

Phone: +81 86 235 6665

Fax: +81 86 235 6669

E-mail: [tmatsu@md.okayama-u.ac.jp](mailto:tmatsu@md.okayama-u.ac.jp)

## Abstract

Bone regeneration was one of the earliest fields to develop in the context of tissue regeneration, and currently, repair of small-sized bone defects has reached a high success rate. Future researches are expected to incorporate more advanced techniques towards achieving rapid bone repair and modulation of the regenerated bone quality. For these purposes, it is important to have a more integrative understanding of the mechanisms of bone formation and maturation from multiple perspectives and to incorporate these new concepts into the development and designing of novel materials and techniques for bone regeneration.

This review focuses on the analysis of the earliest stages of bone tissue development from the biology, material science, and engineering perspectives for a more integrative understanding of bone formation and maturation, and for the development of novel biology-based engineering approaches for tissue synthesis *in vitro*. More specifically, the authors describe the systematic methodology that allowed the understanding of the different nucleation sites in intramembranous and endochondral ossification, the space-making process for mineral formation and growth, as well as the process of apatite crystal cluster growth *in vivo* in the presence of suppressing biomolecules.

## Significance of this paper

This review paper describes the bone formation process re-examined from an engineering point of view. Here, we evaluated the morphological changes on a macro and micro scale as well as changes in the physical and chemical environment in bone tissue development. Through this approach, various new phenomena in bone formation have been clarified, such as the rupture of hypertrophic chondrocytes due to mechanical stimulation and the formation of calcified globules caused by this rupture. These new phenomena were acquired only by examining it from an engineering point of view. In this paper, we will explain in detail these new bone formation processes and the growth mechanism of calcified globules. These mechanisms will provide useful information for the synthesis of new bone-like materials and the production of bone organoids.

## 1. Introduction

Bone tissue is composed of different cell types and a highly complex composite material, which endows it with unique physico-chemical and mechanical properties (e.g., elasticity, force bending, hardness) to attain crucial functions in the body, such as ion homeostasis, organ protection, locomotion, and hematopoiesis (1). The composition, nanostructure, and function of bone, including its constituting cells, have drawn the attention of researchers from different scientific fields, such as biology, chemistry, material science, engineering, and computational sciences (1, 2).

A number of review papers have described in detail the composition and structure of bones (3-5). On the other hand, few are the studies that describe in detail the spatio-temporal changes in bone composition and structure. Not surprisingly, all bones are not composed of 65% minerals, 25% organics, and 10% water from the initial developmental stage. Osteon or the Haversian system, which is often seen in the schemas of review papers, is described as if it is the basic structure of bone, but in fact, this is a microstructure found only in the diaphysis (cortical bone) of mature long bones. Naturally, neither bone apatite nor type I collagen is oriented from the initial bone developmental or regeneration stages. For example, in the case of the regenerated bone, preferential recovery of bone mass is observed in the initial 4 weeks of repair, and thereafter, changes in apatite crystal orientation depend on the subjected mechanical forces (6, 7).

Biomimicking techniques closely reproducing the spatio-temporal changes in bone tissue can allow the development of more sophisticated biodevices that can fill the gap between the *in vitro* and *in vivo* findings. To that end, the knowledge obtained by conventional life science techniques, such as histology, cellular and molecular biology is indeed important. In addition to that, it is crucial to understand how the materials, such as cells, extracellular matrix and the surrounding minerals change in a spatio-temporal manner. Many organic substances show self-organization in the process of tissue development. The type and amount of inorganic minerals also influence the degree of this self-organization. It is also important to understand the physical and chemical properties of the surrounding microenvironment.

The history of using synthetic materials instead of metals to treat bone defects or abnormalities dates back to 1970, when a method for hydroxyapatite synthesis was developed (8-10). Subsequently, organic-inorganic hybrid materials composed of synthesized calcium phosphate and organic substances, such as collagen, have been studied as bone substitute materials (11-13). Onward the 1990s, many bone regeneration studies using osteoblasts and mesenchymal stem cells or reporting the development of materials (e.g., PCL nanofibers, bioglass) to control the differentiation of these cells have been reported (13-22). In recent years, the generation of bone organoids, using cells as material, has become increasingly active (23, 24) (Fig. 1). However, an important issue on the fabrication of bone mimic materials that should be emphasized is related to the fact that the bone tissue is highly dynamic, and our understanding and manipulation of the materials and factors regulating bone tissue formation *in vitro* should also be finely-tuned in a spatio-temporal manner.

Additionally, what has been missing in the *in vitro* reproduction systems using cells was the understanding and utilization of the mineral nucleation factors. From the biology viewpoint, cell-secreted matrix vesicles (MVs) have been reported to be the site where the initial minerals are formed (25, 26). Nevertheless, the exact mechanisms of how MVs calcify have not been clarified. For instance, the mechanisms of how calcium ions enter the MVs to react with phosphate ions have remained unclear. Additionally, the utilization of isolated intact MVs for *in vitro* bone-like tissue formation has been unsuccessful (27). Therefore, before engineering a biomimetic bone tissue *in vitro*, we focused on the understanding of the mechanisms of bone formation *in vivo* based on a minute and systematic analysis from the biology and material science viewpoints.

## 2. The earliest mineralization in calvarial intramembranous ossification

In an attempt to understand the events behind the earliest process of osteoblast-driven intramembranous ossification, we first identified the exact location of the initial mineralization site. In other words, we challenged to investigate the changes in cell morphology and function, extracellular matrix composition and structure associated with the earliest deposition of inorganic material in mouse calvaria from an engineer's viewpoint. To identify the initial mineralization site, mouse calvaria at different

developmental stages were stained with calcein and alizarin red, and the findings were confirmed by micro-computed tomography (micro-CT). As a result, the earliest mineralization in mouse calvaria was found to start in the upper orbit of the frontal bone at embryonic day 14 (E14), and to expand towards the sagittal line on the following hours (E14.5) (Fig. 2).

For a minute analysis of the mineralization site, the trimmed samples were embedded in resin and observed by a scanning electron microscope (SEM) using a back-scattered electron detector and transmission electron microscope (TEM) (28). As a result, we found that the earliest mineralization proceeded through three stages: The initially highly-compacted cells, demonstrated by the expression of intercellular connexin 43 gap junctions, lose cell-cell contact. Concomitant with the decrease in the expression of connexin 43, the expression of integrins and the secretion of collagen fibers are observed at the initial mineralization site. As a result, large gaps, where the minerals will be formed, are created between the cells. The second stage is characterized by the release of large amounts of MVs from the cells into the intercellular space occupied by collagen. Of note, secretion of MVs was seen not to be associated with cellular membrane budding, but most probably with the lysosomal pathway in transporting and secreting intraluminal MVs, similar that of exosomes (29) (Fig. 3).

The third stage involves mineralization inside the MVs, as reported previously (26). Of note, the initial minerals seen by TEM were amorphous calcium phosphate (ACP), which then transformed into low crystalline hydroxyapatite, as detected by electron diffraction. The initial size of the minerals was the same as those of MVs, but after growth, the minerals showed a diameter of less than 1  $\mu\text{m}$  in diameter, which has been previously named as “calcospherites”. A large amount of these minerals are formed in the vicinity of the collagen fibrils, grow and become densely packed, and eventually, go through a maturation stage (28) (Fig. 4). At a macroscopic level, sodium hypochlorite-treated samples revealed that the mineralized area at E14.5 presented a mesh structure, where blood vessels could be found inside, and in the next stages, the mineralized tissue becomes a highly compact mature bone.

### 3. The earliest mineralization in the epiphyseal endochondral ossification

Long bones are known to be formed through a process named endochondral ossification, which involves mainly the activity of chondrocytes. Using the same systematic methods described in section 2, we were able to identify the initial mineralization site in the medial side of mouse femur epiphysis at post-natal day 5.5 (P5.5), where numerous chondrocytes had become hypertrophic. The initial approach to try to understand the initial mineralization events was again to examine how the mineralization space could be formed inside the cell-rich and highly dense cartilage matrix. For that purpose, the *ex vivo* isolated epiphyses at P6 were observed using a time-lapse microscope. Surprisingly, we found that hypertrophic chondrocytes near the mineralized area burst and shrunk, promoting space for mineral formation (30). At this site, oppositely to the space formed by the osteoblasts by collagen deposition during intramembranous ossification, the space was formed by the death of chondrocytes, which shrunk and allowed the cartilage matrix, including collagens, to expand to the area previously occupied by the hypertrophic chondrocytes (Fig. 5).

Further detailed analysis of the initial mineralization area by backscattered electron-mode SEM revealed no MVs, but numerous nanosized fragments as the nucleation site for mineral formation in the surroundings of the hypertrophic chondrocytes (Fig. 6). Elemental mapping of these fragments further demonstrated that they were rich in phosphorus and osmium, which strongly binds to lipids. Therefore, we assumed that the fragments were phospholipids from the cell membrane, and termed them as “cell membrane nanofragments” (31). In fact, the association of phospholipids in bone formation had been previously reported (32).

We also assumed that the cell membrane nanofragments were formed by the burst of the hypertrophic chondrocytes. In other words, after the hypertrophic chondrocytes burst and shrunk, parts of the cell membrane could be remained tightly attached to the extracellular matrix and would give origin to the nanofragments. To test this hypothesis, chemical (osmotic pressure, pH) and mechanical cues were applied to the *ex vivo* isolated mouse epiphysis and the number of chondrocyte burst were counted using the time-lapse videos. Interestingly, chondrocyte bursts were shown to be modulated by high mechanical



pressure, hypotonic solution, and alkaline pH (30, 33). Higher chondrocyte burst events were associated with the presence of higher amounts of cell membrane nanofragments. Of note, when the lower limb of newborn mice was immobilized to avoid the body pressure onto the joints, bone formation in the epiphysis was shown to be delayed, suggesting that the mechanical pressure would be necessary for chondrocyte burst, which would give origin to the cell membrane nanofragments, which in turn would be the nucleation site for mineral formation.

Qualitative analysis indicated that the initial minerals formed from the cell membrane nanofragments were shown to be ACP, which then subsequently transformed into low crystalline apatite, forming clusters of more than 1  $\mu\text{m}$  in diameter. A large number of minerals were formed in the surroundings of the dead chondrocytes, filling completely the space between the cells, and subsequently, became more densely packed forming the trabecular bone.

On the other hand, unlike the calvaria, the mineralized region expanded only through the space between the cells, resulting in concave non-calcified regions, which would be transformed into a myelopoietic site in the following stages. Of note, ossification at the femur epiphysis (secondary ossification) shows different stages and processes compared with that at the femur diaphysis (primary ossification), which involves both cortical and cancellous bone formation.

#### **4. Understanding of the microenvironment of initial mineral formation**

As described in the previous sections, the earliest process of mineralization of the calvaria and femur epiphyses involve: a) space-making for mineralization, b) nucleation and formation of mineralization precursors, c) mineral growth, maturation, and formation of small calcospherites, and d) aggregation of calcospherites into large calcified bodies. In particular, the detailed understanding of the nucleation sites and initial calcospherite formation has a critical role in bone biomimicking, and importantly, these processes can be described in terms of chemical reactions between biomolecules and inorganic ions.

X-ray diffraction and electron diffraction have shown that the initial minerals formed from either MVs or cell membrane nanofragments were ACP, which then transformed into

acicular apatite crystals that have grown radially. The chemical environment of the surroundings is critical for mineral precipitation and defines the actual crystal growth speed, size, and morphology.

Since the report of wet artificial synthesis methods of hydroxyapatite (HAp) in the 1970s, synthesis of HAp at different pHs or by adding specific molecules became highly controllable and allowed a deeper understanding of the chemical processes involved in ion nucleation and precipitation, and crystal growth (34, 35). In these systems, the HAp precursors, octacalcium phosphate (OCP), and ACP (36) are known to be produced in a pH 7 or lower and alkaline pH, respectively (37, 38) (Fig. 7). ACP appears to be the predominant precursor of mineralization in the observed initial mineralization sites in calvaria and femur epiphysis. To understand the *in vivo* microenvironment, we directly measured the pH of the initial mineralization region and found it to be alkaline (around 8.5) (33), which confirmed the previous hypothesis (39) (Fig. 8). Importantly, phosphate ion-releasing enzymes such as alkaline phosphatases (ALP), which become highly expressed before the initial mineralization takes place, have their optimal pKa activity in an alkaline condition (around 8.5 to 9.5) (41). Since ALPs are known to be anchored to the cell membrane by glycosylphosphatidylinositol (42), incubation of cell membrane nanofragments *in vitro* in an alkaline pH (8.5) could remarkably promote their mineralization, which occurred within 1 day.

Alkaline pH has also important roles in ion precipitability and crystal growth (43). An alkaline pH would favor a high precipitability of [Ca] and [P] ions and eventual mineral nucleation (formation of mineralization precursors). In fact, HAp mineral precipitation is facilitated in alkaline conditions (33). Moreover, in alkaline conditions, anisotropic or weak-anisotropic growth favors the formation of spherical HAp clusters. On the other hand, acidic pH favors a low precipitability of the ions and precipitation in the already existing minerals, subsequently promoting crystal growth. The anisotropic growth in an acidic environment would promote the formation of large rods or plates (33). A major notion behind this concept is that pH intimately affects ion solubility, which consequently, determines the direction of many reactions, including dissolution, precipitation, and phase transformation (44). Most calcium phosphates, including HAp, shows a high solubility (and

less precipitability) in acidic conditions, and that decreases proportionally to the increase in pH, until pH 8 to 9 (44-46). Additionally, theoretical equations can also provide estimations of the interfacial free energies of minerals and the kinetic coefficients for nucleation, and have shown that the nucleation rates of HAp indeed increase with increasing pH (47). Of note, the presence of nucleation sites significantly reduces the activation energy, and the nucleation rate is increased accordingly (48).

## 5. Roles of water in initial crystal growth

Numerous studies have investigated the interaction of HAp with many organic substances, such as collagen, acidic amino acids, and acidic proteins such as small integrin-binding ligand, N-linked glycoproteins (SIBLINGs) (49-53). Due to their high affinity, these abovementioned proteins strongly bind to HAp crystals and inhibit their growth (54, 55). Nevertheless, the initial minerals “calcospherites” formed in intramembranous or endochondral ossification were uniform in size. In other words, up to a certain size, it may be possible that organic molecules might not inhibit HAp crystal growth. Therefore, we investigated the important factors determining biomolecule adhesion to HAp crystal and found the critical roles of apatite-ion replacement and water in determining organic molecule adhesion and crystal growth.

HAp has a chemical formula of  $\text{Ca}_{10}(\text{PO}_4)_6(\text{OH})_2$  and is composed of Ca, P, O, and H. In bone tissue, HAp is replaced by various small elements, such as cations ( $\text{Mg}^{2+}$ ,  $\text{Sr}^{2+}$ ,  $\text{Zn}^{2+}$ ) and anions ( $\text{CO}_3^{2-}$ ,  $\text{SO}_4^{2-}$ ) (56-58), which can induce crystal strain. To understand the relationship between HAp crystals and water during its growth, we synthesized HAp substituted with various cations and investigated the existence of non-freezing, intermediate, and free water on the crystal. As a result, it was shown that the substitution of Mg ion decreased the surface free energy of HAp crystal and, more importantly, increased the amount of intermediate water. Intermediate water has been paid special attention because of its role in suppressing protein adsorption (59). In fact, the increased amount of intermediate water due to Mg-substitution caused a marked suppression of the amount of protein adsorption onto HAp (60).

Of note, the crystal size of Mg-substituted HAp was significantly larger than those synthesized without Mg ions. An *in vivo* experiment, where mice were maintained on a Mg-rich or Mg-absent diet, further confirmed the *in vitro* findings. In other words, unlike artificial synthesis of HAp, the HAp crystal growth *in vivo* is not suppressed even in an environment abundant in organic molecules. Therefore, the HAp crystal is able to grow to a uniform size. Considering this result and the hydration state around the HAp crystals, it seemed that the presence of intermediate water between the inter-crystal spaces prevents the invasion of organics, such as proteins (Fig. 9).

On the other hand, the formed apatite crystals contact each other and finally aggregate to form dense mineralized lumps without gaps. Crystal aggregation at this stage could be associated with apatite dehydration, although further investigation is required to obtain more details.

## 6. Conclusion and future perspectives

This review summarizes the current findings in the chemical and material aspects of the earliest stages of bone development, especially the space-making process, nucleation sites, and apatite crystal formation and growth (Fig. 10). In accordance with previous results, MVs certainly play important roles in the initial calvarial intramembranous ossification. On the other hand, the cellular membrane nanofragments are important components for the initial mineralization in the femur epiphysis.

A close investigation of the actual mineralization shows that both intramembranous and endochondral ossification may occur in a semi-closed confined space around the cells. In this semi-closed space, mineralization is controlled by the interaction between organics and inorganics. Moreover, once mineralization occurs, the amount of minerals increases at an accelerating rate, which would limit the size of calcospherites, but, in fact, the mineral growth in the initial development stage was not markedly affected by collagen and non-collagenous proteins *in vivo*. In addition, we assume that crystal growth occurs while organics, such as proteins, are removed at the confined nano-environment. This concept is in contradiction with the past hypotheses showing that minerals precipitate and grow in the gap between collagen fibrils (61, 62).

Nevertheless, several aspects still remain unclear. For instance, how do apatite crystals form agglomerates in the presence of suppressing organics? To what extent are these crystals remodeled, and how will the remodeling result in complexation with organics, such as collagen? Questions also remain regarding how the apatite crystals exhibit anisotropy under the influence of mechanical stimuli. Future studies are still necessary to unravel the detailed complexity of bone formation and maturation.

In summary, the understanding of the initial bone formation from an engineering perspective is important not only for more precise control of the bone quality of generated bone or bone organoids but also for the design of new therapeutic methods.

### **Acknowledgments**

This research was funded by JSPS KAKENHI grant numbers JP20H04534, JP19H03837, JP20H05225, and JP18H05254, as well as by the Iketani Science and Technology Foundation grant number 0321025-A.

### **Competing financial interests**

All authors declare that there are no competing financial interests.

## References

1. Bilezikian, J.P., Martin, T.J., Clemens, T., *et al.* Principles of bone biology. 4th edition Cambridge: Academic Press; 2019.
2. Vallet-Regi, M, Navarrete, D. Biological apatites in bone and teeth. Nanoceramics in clinical use: From materials to applications (2): The Royal Society of Chemistry; 2016. pp. 1.
3. Usami, Y., Gunawardena, A.T., Iwamoto, M., and Enomoto-Iwamoto, M. Wnt signaling in cartilage development and diseases: lessons from animal studies. *Lab Invest* **96**, 186, 2016.
4. Nair, A.K., Gautieri, A., Chang, S.W., and Buehler, M.J. Molecular mechanics of mineralized collagen fibrils in bone. *Nat Commun* **4**, 1724, 2013.
5. Tertuliano, O.A., and Greer, J.R. The nanocomposite nature of bone drives its strength and damage resistance. *Nat Mater* **15**, 1195, 2016.
6. Nakano, T., Kaibara, K., Ishimoto, T., Tabata, Y., and Umakoshi, Y. Biological apatite (BAP) crystallographic orientation and texture as a new index for assessing the microstructure and function of bone regenerated by tissue engineering. *Bone* **51**, 741, 2012.
7. Ishimoto, T., Nakano, T., Umakoshi, Y., Yamamoto, M., and Tabata, Y. Degree of biological apatite c-axis orientation rather than bone mineral density controls mechanical function in bone regenerated using recombinant bone morphogenetic protein-2. *J Bone Miner Res* **28**, 1170, 2013.
8. Elliott, J.C., Mackie, P.E., and Young, R.A. Monoclinic hydroxyapatite. *Science* **180**, 1055, 1973.
9. Neuman, W.F., and Mulryan, B.J. Synthetic hydroxyapatite crystals. 3. The carbonate system. *Calcif Tissue Res* **1**, 94, 1967.
10. Neman, W.F., Toribara, T.Y., and Mulryan, B.J. Synthetic hydroxyapatite crystals. 1. Sodium and potassium fixation. *Arch Biochem Biophys* **98**, 384, 1962.
11. Hahn, E., Sonis, S., Gallagher, G., and Atwood, D. Preservation of the alveolar ridge with hydroxyapatite-collagen implants in rats. *J Prosthet Dent* **60**, 729, 1988.

12. Okazaki, M., Ohmae, H., Takahashi, J., Kimura, H., and Sakuda, M. Insolubilized properties of UV-irradiated CO<sub>3</sub> apatite-collagen composites. *Biomaterials* **11**, 568, 1990.
13. Lee, K.Y., Alsberg, E., and Mooney, D.J. Degradable and injectable poly(aldehyde guluronate) hydrogels for bone tissue engineering. *J Biomed Mater Res* **56**, 228, 2001.
14. Crane, G.M., Ishaug, S.L., and Mikos, A.G. Bone tissue engineering. *Nat Med* **1**, 1322, 1995.
15. Ishaug-Riley, S.L., Crane, G.M., Gurlek, A., Miller, M.J., Yasko, A.W., Yaszemski, M.J., and Mikos, A.G. Ectopic bone formation by marrow stromal osteoblast transplantation using poly(DL-lactic-co-glycolic acid) foams implanted into the rat mesentery. *J Biomed Mater Res* **36**, 1, 1997.
16. Schoeters, G.E., de Saint-Georges, L., Van den Heuvel, R., and Vanderborght, O. Mineralization of adult mouse bone marrow in vitro. *Cell Tissue Kinet* **21**, 363, 1988.
17. Meka, S.R.K., Agarwal, V., and Chatterjee, K. In situ preparation of multicomponent polymer composite nanofibrous scaffolds with enhanced osteogenic and angiogenic activities. *Mater Sci Eng C Mater Biol Appl* **94**, 565, 2019.
18. Meng, D., Rath, S.N., Mordan, N., Salih, V., Kneser, U., and Boccaccini, A.R. In vitro evaluation of 45S5 Bioglass-derived glass-ceramic scaffolds coated with carbon nanotubes. *J Biomed Mater Res A* **99**, 435, 2011.
19. Woodruff, M.A., Rath, S.N., Susanto, E., Haupt, L.M., Hutmacher, D.W., Nurcombe, V., and Cool, S.M. Sustained release and osteogenic potential of heparan sulfate-doped fibrin glue scaffolds within a rat cranial model. *J Mol Histol* **38**, 425, 2007.
20. Meka, S.R.K., Verma, S.K., Agarwal, V., and Chatterjee, K. In situ silication of polymer nanofibers to engineer multi-biofunctional composites. *Chemistryselect* **3**, 3762, 2018.
21. Bartold, M., Gronthos, S., Haynes, D., and Ivanovski, S. Mesenchymal stem cells and biologic factors leading to bone formation. *J Clin Periodontol* **46 Suppl 21**, 12, 2019.

22. Kingery, M.T., Manjunath, A.K., Anil, U., and Strauss, E.J. Bone marrow mesenchymal stem cell therapy and related bone marrow-derived orthobiologic therapeutics. *Curr Rev Musculoskelet Med* **12**, 451, 2019.
23. Sasaki, J., Asoh, T.A., Matsumoto, T., Egusa, H., Sohmura, T., Alsberg, E., Akashi, M., and Yatani, H. Fabrication of three-dimensional cell constructs using temperature-responsive hydrogel. *Tissue Eng Part A* **16**, 2497, 2010.
24. Sasaki, J., Matsumoto, T., Egusa, H., Matsusaki, M., Nishiguchi, A., Nakano, T., Akashi, M., Imazato, S., and Yatani, H. In vitro reproduction of endochondral ossification using a 3D mesenchymal stem cell construct. *Integr Biol (Camb)* **4**, 1207, 2012.
25. Ali, S.Y., Sajdera, S.W., and Anderson, H.C. Isolation and characterization of calcifying matrix vesicles from epiphyseal cartilage. *Proc Natl Acad Sci U S A* **67**, 1513, 1970.
26. Anderson, H.C. Vesicles associated with calcification in the matrix of epiphyseal cartilage. *J Cell Biol* **41**, 59, 1969.
27. Boskey, A.L., Boyan, B.D., Doty, S.B., Feliciano, A., Greer, K., Weiland, D., Swain, L.D., and Schwartz, Z. Studies of matrix vesicle-induced mineralization in a gelatin gel. *Bone Miner* **17**, 257, 1992.
28. Kunitomi, Y., Hara, E.S., Okada, M., Nagaoka, N., Kuboki, T., Nakano, T., Kamioka, H., and Matsumoto, T. Biomimetic mineralization using matrix vesicle nanofragments. *J Biomed Mater Res A* **107**, 1021, 2019.
29. Iwayama, T., Okada, T., Ueda, T., Tomita, K., Matsumoto, S., Takedachi, M., Wakisaka, S., Noda, T., Ogura, T., Okano, T., Fratzl, P., Ogura, T., and Murakami, S. Osteoblastic lysosome plays a central role in mineralization. *Sci Adv* **5**, eaax0672, 2019.
30. Hara, E.S., Okada, M., Nagaoka, N., Hattori, T., Iida, L.M., Kuboki, T., Nakano, T., and Matsumoto, T. Chondrocyte burst promotes space for mineral expansion. *Integr Biol (Camb)* **10**, 57, 2018.
31. Hara, E.S., Okada, M., Nagaoka, N., Hattori, T., Kuboki, T., Nakano, T., and Matsumoto, T. Bioinspired mineralization using chondrocyte membrane nanofragments. *Acs Biomater Sci Eng* **4**, 617, 2018.

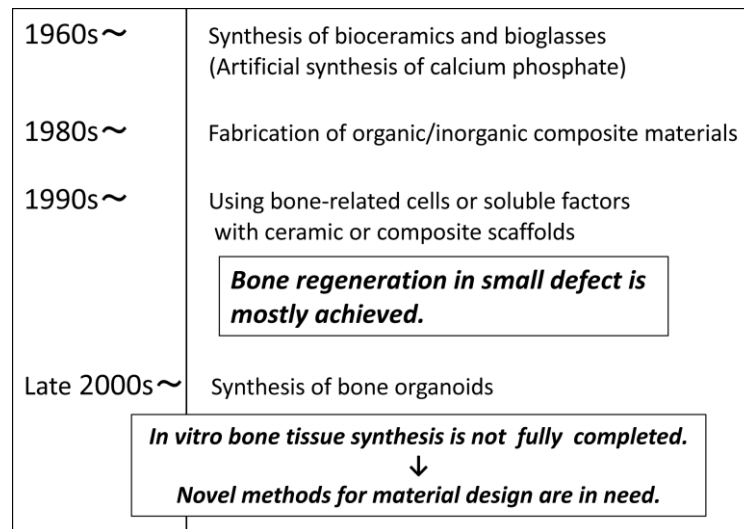


32. Irving, J.T. A histological stain for newly calcified tissues. *Nature* **181**, 704, 1958.
33. Hara, E.S., Okada, M., Kuboki, T., Nakano, T., and Matsumoto, T. Rapid bioinspired mineralization using cell membrane nanofragments and alkaline milieu. *J Mater Chem B* **6**, 6153, 2018.
34. Matsumoto, T., Okazaki, M., Inoue, M., Hamada, Y., Taira, M., and Takahashi, J. Crystallinity and solubility characteristics of hydroxyapatite adsorbed amino acid. *Biomaterials* **23**, 2241, 2002.
35. Matsumoto, T., Okazaki, M., Inoue, M., Yamaguchi, S., Kusunose, T., Toyonaga, T., Hamada, Y., and Takahashi, J. Hydroxyapatite particles as a controlled release carrier of protein. *Biomaterials* **25**, 3807, 2004.
36. Wang, Y.W., Christenson, H.K., and Meldrum, F.C. Confinement increases the lifetimes of hydroxyapatite precursors. *Chem Mater* **26**, 5830, 2014.
37. Saxton, C.A. Identification of octacalcium phosphate in human dental calculus by electron diffraction. *Arch Oral Biol* **13**, 243, 1968.
38. Suzuki, O. Octacalcium phosphate: osteoconductivity and crystal chemistry. *Acta Biomater* **6**, 3379, 2010.
39. Brandao-Burch, A., Utting, J.C., Orriss, I.R., and Arnett, T.R. Acidosis inhibits bone formation by osteoblasts in vitro by preventing mineralization. *Calcif Tissue Int* **77**, 167, 2005.
40. Kumpulainen, T. Immunohistochemical localization of human carbonic anhydrase isozymes. *Ann N Y Acad Sci* **429**, 359, 1984.
41. Millan, J.L. Alkaline Phosphatases : Structure, substrate specificity and functional relatedness to other members of a large superfamily of enzymes. *Purinergic Signal* **2**, 335, 2006.
42. Chakrabartty, A., and Stinson, R.A. Properties of membrane-bound and solubilized forms of alkaline phosphatase from human liver. *Biochim Biophys Acta* **839**, 174, 1985.

43. Sadat-Shojai, M., Khorasani, M.T., Dinpanah-Khoshdargi, E., and Jamshidi, A. Synthesis methods for nanosized hydroxyapatite with diverse structures. *Acta Biomater* **9**, 7591, 2013.
44. Chow, L.C. Solubility of calcium phosphates. *Monogr Oral Sci* **18**, 94, 2001.
45. Brown, W.E. Solubilities of phosphates and other sparingly soluble compounds. *Environmental phosphorus handbook*. New York: Wiley; 1973. pp. 203.
46. Nancollas, G.H., and Koutsoukos, P.G. Calcium-phosphate nucleation and growth in solution. *Prog Cryst Growth Ch* **3**, 77, 1980.
47. Boistelle, R., and Lopezvalero, I. Growth units and nucleation - the case of calcium phosphates. *J Cryst Growth* **102**, 609, 1990.
48. Meyers, M.A., and Chen, P.Y. *Biological materials science: biological materials, bioinspired materials, and biomaterials*. Cambridge: Cambridge University Press; 2014.
49. Cutini, M., Corno, M., Costa, D., and Ugliengo, P. How does collagen adsorb on hydroxyapatite? Insights from ab initio simulations on a polyproline type II model. *J Phys Chem C* **123**, 7540, 2019.
50. Kikuchi, M., Itoh, S., Ichinose, S., Shinomiya, K., and Tanaka, J. Self-organization mechanism in a bone-like hydroxyapatite/collagen nanocomposite synthesized in vitro and its biological reaction in vivo. *Biomaterials* **22**, 1705, 2001.
51. Boskey, A.L., Christensen, B., Taleb, H., and Sorensen, E.S. Post-translational modification of osteopontin: effects on in vitro hydroxyapatite formation and growth. *Biochem Biophys Res Commun* **419**, 333, 2012.
52. Staines, K.A., MacRae, V.E., and Farquharson, C. The importance of the SIBLING family of proteins on skeletal mineralisation and bone remodelling. *J Endocrinol* **214**, 241, 2012.
53. Milan, A.M., Sugars, R.V., Embery, G., and Waddington, R.J. Adsorption and interactions of dentine phosphoprotein with hydroxyapatite and collagen. *Eur J Oral Sci* **114**, 223, 2006.

54. Hunter, G.K., Hauschka, P.V., Poole, A.R., Rosenberg, L.C., and Goldberg, H.A. Nucleation and inhibition of hydroxyapatite formation by mineralized tissue proteins. *Biochem J* **317** ( Pt 1), 59, 1996.
55. Romberg, R.W., Werness, P.G., Riggs, B.L., and Mann, K.G. Inhibition of hydroxyapatite crystal growth by bone-specific and other calcium-binding proteins. *Biochemistry* **25**, 1176, 1986.
56. Bigi, A., Boanini, E., Capuccini, C., and Gazzano, M. Strontium-substituted hydroxyapatite nanocrystals. *Inorg Chim Acta* **360**, 1009, 2007.
57. Okazaki, M., Moriwaki, Y., Aoba, T., Doi, Y., and Takahashi, J. Solubility behavior of CO<sub>3</sub> apatites in relation to crystallinity. *Caries Res* **15**, 477, 1981.
58. Okazaki, M., Miake, Y., Tohda, H., Yanagisawa, T., Matsumoto, T., and Takahashi, J. Functionally graded fluoridated apatites. *Biomaterials* **20**, 1421, 1999.
59. Tanaka, M., Hayashi, T., and Morita, S. The roles of water molecules at the biointerface of medical polymers. *Polym J* **45**, 701, 2013.
60. Okada, M., Hara, E.S., Kobayashi, D., Kai, S., Ogura, K., Tanaka, M., and Matsumoto, T. Intermediate water on calcium phosphate minerals: Its origin and role in crystal growth. *ACS Applied Bio Materials* **2**, 981, 2019.
61. Glimcher, M.J. Molecular biology of mineralized tissues with particular reference to bone. *Rev Mod Phys (RMP)* **31**, 359, 1959.
62. Midura, R.J., Vasanji, A., Su, X., Wang, A., Midura, S.B., and Gorski, J.P. Calcospherulites isolated from the mineralization front of bone induce the mineralization of type I collagen. *Bone* **41**, 1005, 2007.

## Figure Legends



### Exploring bone tissue synthesis

**Figure 1**

Historical overview of how the research on the synthesis of bone-like materials and bone tissue regeneration has progressed. In recent years, *in vitro* synthesis of bone tissue has been largely studied.

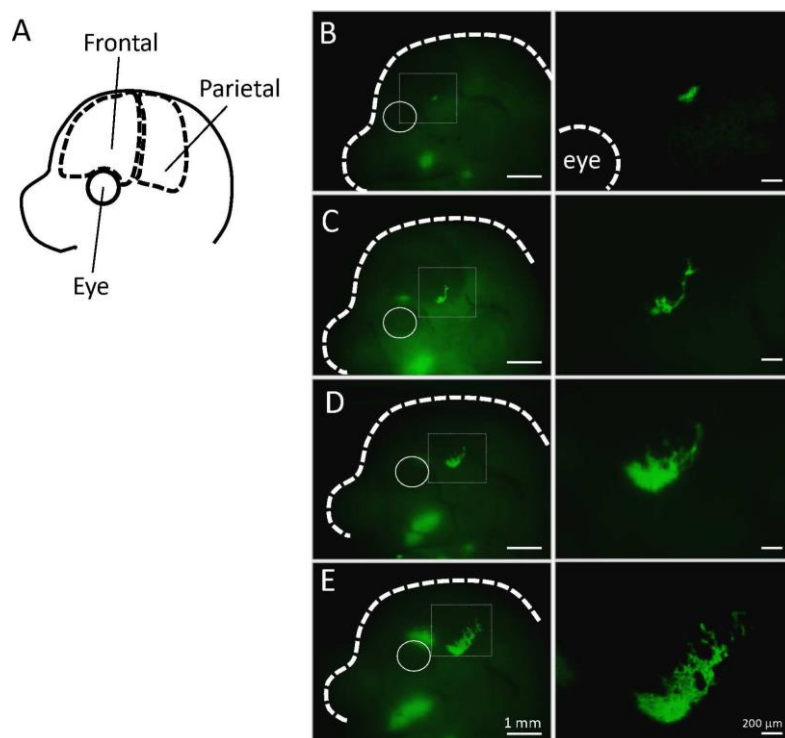


Fig. 2

## Figure 2

Initial mineralization site and growth of frontal and parietal bones in the fetal period. The earliest calcified region found in the upper part of the eye expands toward the parietal region. (Reproduced from Ref. 28 with permission from Wiley.)

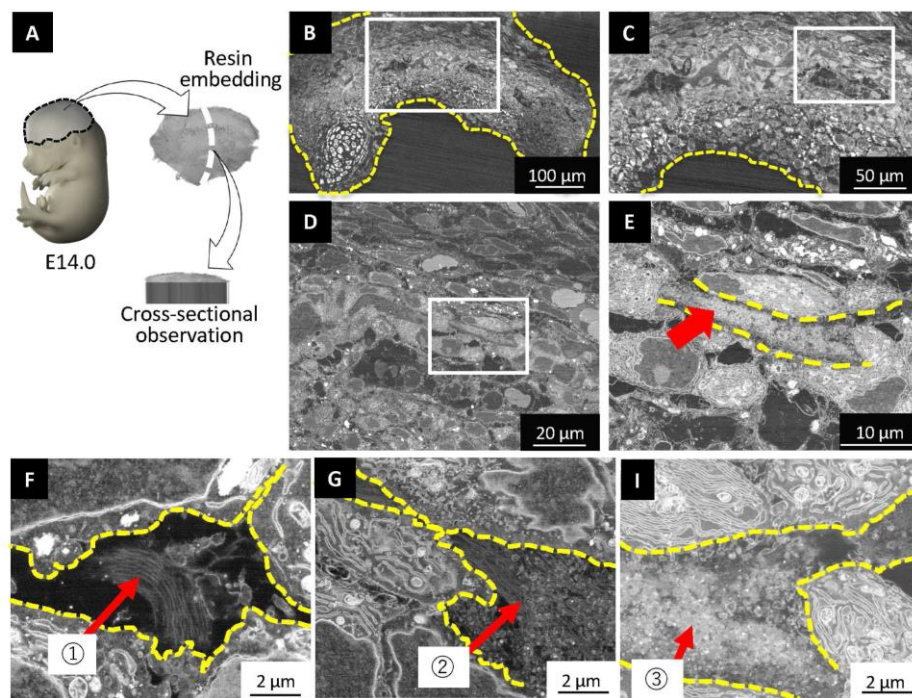


Fig. 3

### Figure 3

(A-E) SEM cross-sectional images of the earliest mineralization site in frontal and parietal bones extracted from E14 embryos. (F) The synchronized states of the earliest mineralization site. First, ① collagen fibers are released from cells into the resulting in intercellular space formation. (G) Matrix vesicles ② are released from the cells. (H) Calcification ③ progresses gradually. (Reproduced from Ref. 28 with permission from Wiley.

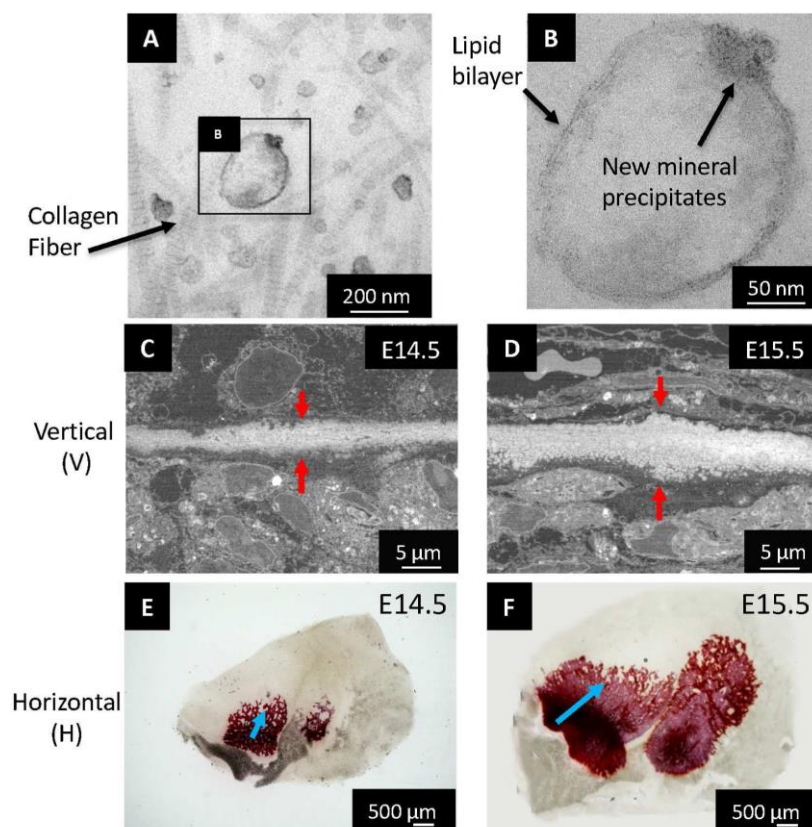


Fig. 4

**Figure 4**

A, B) Calcification in the released matrix vesicles. C-F) The mineralized region expands, but while the growth in the horizontal direction is remarkable (E, F), little growth occurs in the vertical direction (C, D). As a result, a flat bone is formed covering the entire skull.

(Reproduced from Ref. 28 with permission from Wiley.)

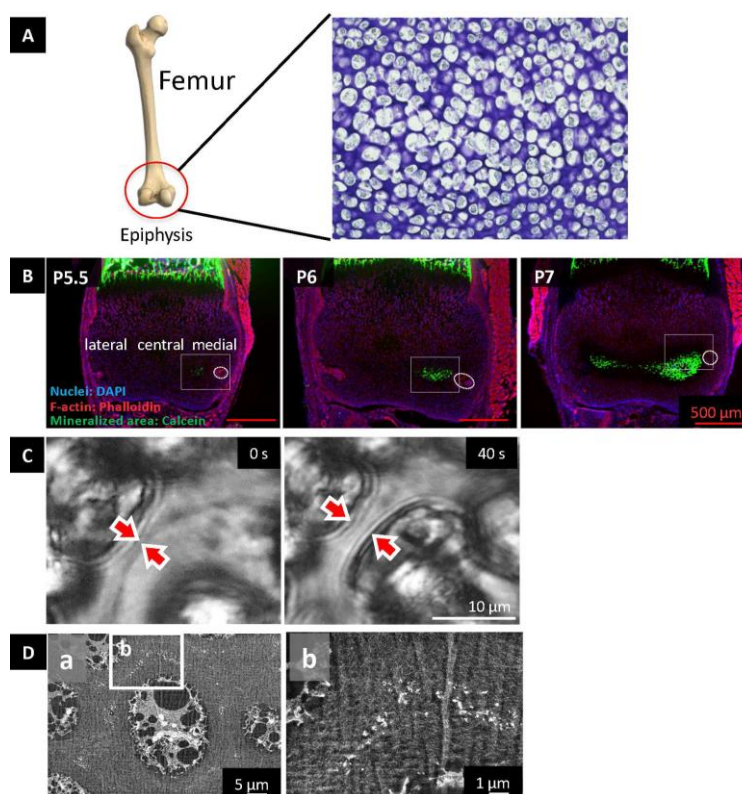


Fig. 5

### Figure 5

A) Figure showing the femur epiphysis, and hypertrophic chondrocytes (large whitish cells) at the early stage of mineralization in mouse femur epiphysis. B) The earliest mineralization is observed at post-natal day 5.5 (P5.5), slightly at the medial region (white square frame). C) Hypertrophic chondrocytes burst and shrink, allowing a space making between chondrocytes, where the initial minerals are deposited. D) As the cell contracts, some cell membrane fragments remain tightly attached to the extracellular matrix around the cells, and these fragments become the nucleation site for mineral formation. (Reproduced from Ref. 30 with permission from the Royal Society of Chemistry.)



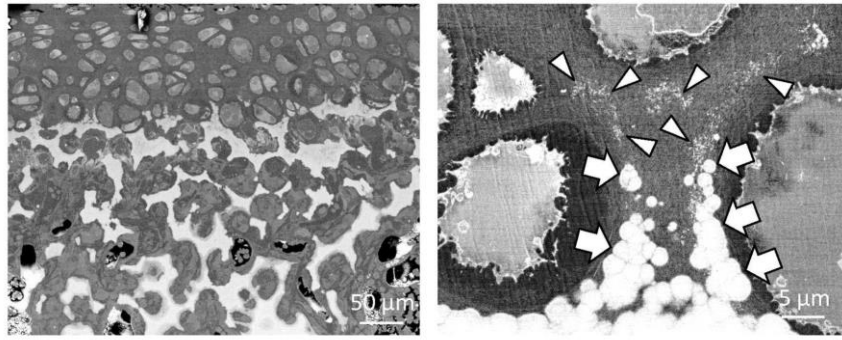


Fig. 6

**Figure 6**

Initial minerals (calcospherites, arrows) were formed by the activity of the remaining cell membrane fragments (arrowheads), which were the nucleation site for mineral formation. As a result of the formation, growth, and fusion of calcospherites, the calcified region expanded.

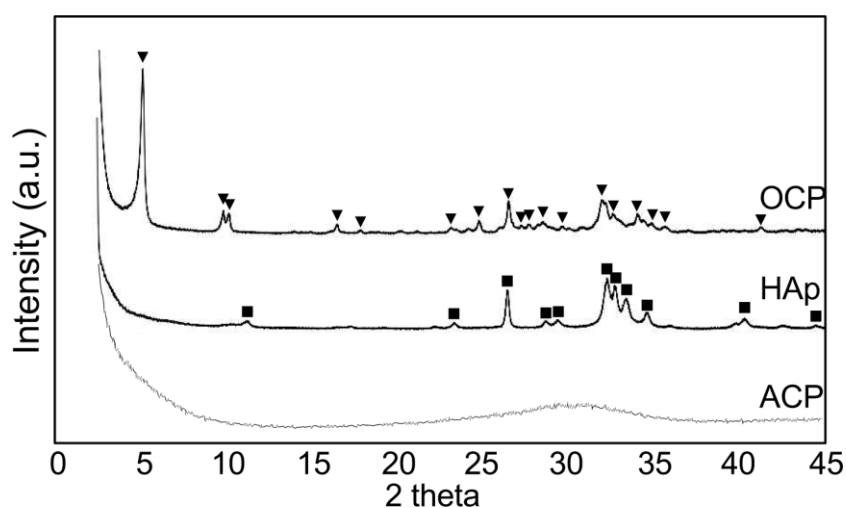


Fig. 7

### Figure 7

XRD patterns of hydroxyapatite (HAp) precursors: octacalcium phosphate (OCP) and amorphous calcium phosphate (ACP). OCP and ACP were synthesized by wet chemical methods using  $\text{Ca}(\text{NO}_3)_2 \cdot \text{H}_2\text{O}$  and  $(\text{NH}_4)_2\text{HPO}_4$  solutions at pH 6.0 (37°C) and pH 11.0 (25°C), respectively. Note the peak at  $4.7^\circ$  ( $2\theta$ ), which characteristic of OCP. ACP shows a broad diffraction with a maximum at approximately  $30^\circ$  ( $2\theta$ ).

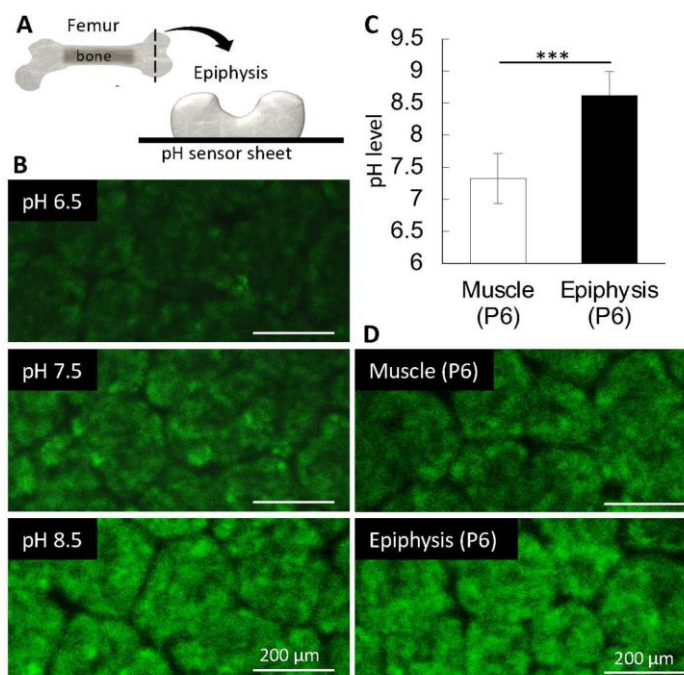


Fig. 8

## Figure 8

A, B) The fluorescent intensity of the pH sensor sheet changes according to the pH. The higher the pH the higher the fluorescent intensity. C, D) Muscle (P6) shows a pH near 7.4, while the epiphysis (P6) shows a pH near 8.5. Graph in (C) shows the quantitative analysis of the fluorescent intensity performed with ImageJ. (Reproduced from Ref. 33 with permission from the Royal Society of Chemistry.)

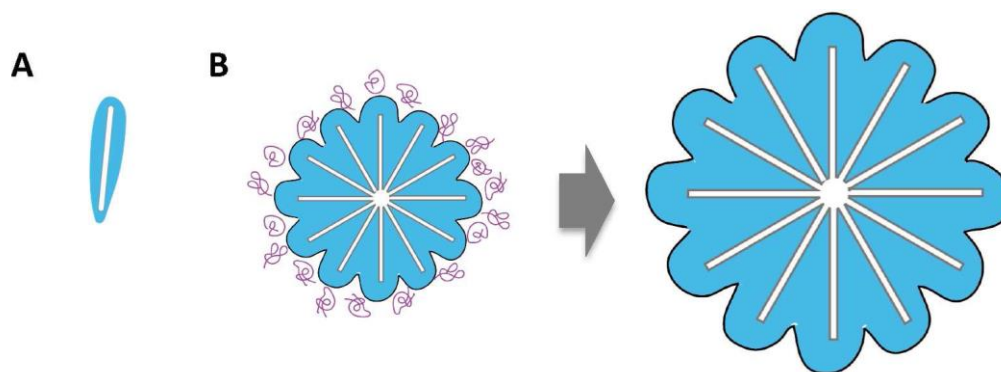
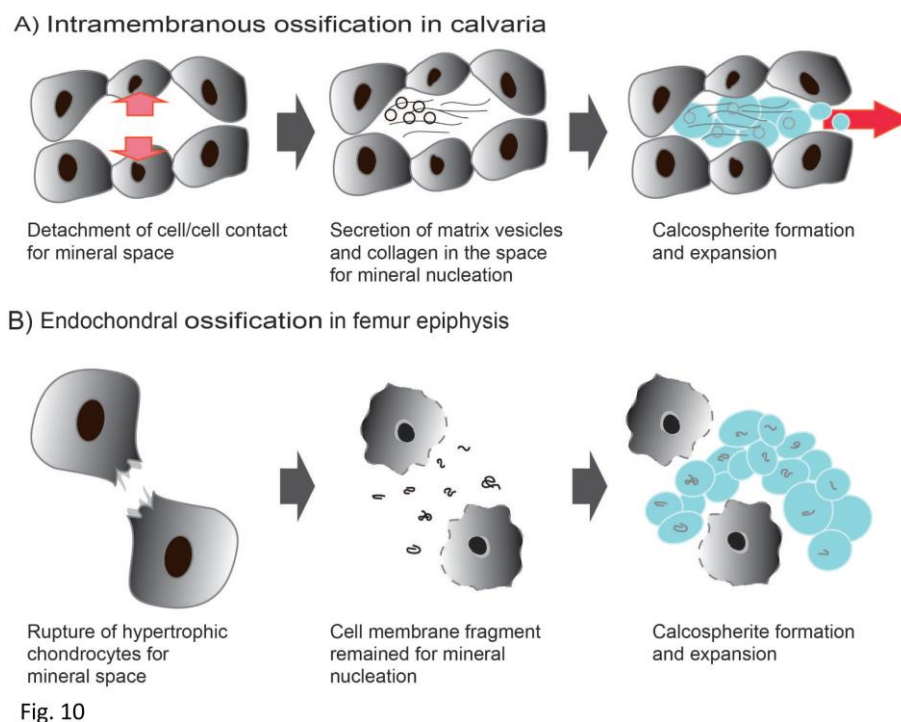


Fig. 9

### Figure 9

A) Single HAp crystal surrounded by intermediate water. B) As a result of the suppression of protein adsorption by the surrounding intermediate water, a uniform calcospherite growth is observed.



**Figure 10**

Schematic illustration of initial mineral formation in each ossification. A) Intramembranous ossification in calvaria. B) Endochondral ossification in femur epiphysis.